Flanders
State of
the Art

20_098_1
FHR reports

IMMERSE Work Package 3.2

Model simulations for Scenario 4

DEPARTMENT
MOBILITY &
PUBLIC
WORKS

www.flandershydraulicsresearch.be

IMMERSE Work Package 3.2

Model simulations for Scenario 4

Stark, J.; Smolders, S.; Plancke, Y.

Flanders Hydraulics Research

Flanders State of the Art

Legal notice

Copyright and citation

D/2022/3241/066

This publication should be cited as follows:

Stark, J.; Smolders, S.; Plancke, Y. (2022). IMMERSE Work Package 3.2: Model simulations for Scenario 4. Version 3.0. FHR Reports, 20_098_1. Flanders Hydraulics Research: Antwerp

Document identification

Customer:	DMOW-aMT	Ref.:	WL2022R20_098_1
Keywords (3-5):	Tides, Sedimentation, Scheldt Estuary, Data analysis		
Knowledge domains:	Hydrodynamics > Tides > Numerical modelling Sediment > Cohesive sediment > Numerical modelling		
Text (p.):	25	Appendices (p.):	7
Confidentiality:	☒ No	☒ Available online	

Author(s):	Stark, J.

Control

	Name	Signature
Reviser(s):	Smolders, S.	Getekend door:Sven Smolders (Signature Getekend op:2022-04-11 13:33:29 +02:0 Reden:Ik keur dit document goed Sven Smolders
Project leader:	Plancke, Y.	Getekend door:Yves Plancke (Signature) Getekend op:2022-06-03 11:54:29 +02:0 Reden:Ik keur dit document goed Yves Plancke

Approval

Head of Division:	Bellafkih, K.	Getekend door:Abdelkarim Bellafkih (Sign Getekend op:2022-04-05 10:29:28 +02:0 Reden:Ik keur dit document goed Abdelkarim Bellafkih

CERTIFIED ISO 9001

Abstract

Flanders Hydraulics Research was asked to apply a recently improved version of the cohesive sediment transport model in Delft3D-NeVla to analyze the impact of the bathymetric changes in the so-called Scenario 4 on the SSC distribution along the Scheldt estuary. In Scenario 4, developed by IMDC as part of the Interreg project IMMERSE’s Work Package 3.2, the bathymetry of the river banks in between Burcht and Rupelmonde just upstream of Antwerp (Lower Sea Scheldt) are raised to a maximum elevation of -1,0 m TAW. Based on the model results, the bathymetric changes in Scenario 4 lead to a SSC reduction of up to 10% in the Lower Sea Scheldt and a SSC increase of 10-40% in the Upper Sea Scheldt for a low discharge situation. This also corresponds to an upward movement of the ETM by about 10 km. The modelled impact during high discharge conditions is much smaller (i.e., relative change in SSC varies between -6% and +8%), as the spatial SSC variation hardly differs between Scenario 4 and the reference scenario for high discharge runs. Regarding the modelled influence on tidal hydrodynamics, Scenario 4 induces a tidal range reduction in the Upper Sea Scheldt, while the shape of the tidal wave becomes slightly more flood dominant upstream of the bathymetric changes and a bit less flood-dominant along and downstream of the altered section.

Contents

List of Tables

List of Figures

1 Introduction

1.1 Problem description

In the context of the Interreg project IMMERSE (Implementing Measures for Sustainable Estuaries), Flanders Hydraulics Research was asked to model the impact of one specific sand disposal scenario on suspended sediment concentrations in the Scheldt Estuary and provide the model output to the University of Antwerp for their ecosystem model. This modeling exercise is part of IMMERSE Work Package 3.2.

IMMERSE WP3.2 - Scenario 4

Previously, IMDC has investigated the potential for large scale strategic disposal of sand along the Sea Scheldt with the purpose to reduce the tidal range along the upstream part of the estuary (IMDC, 2020). They assessed the impact of such large scale interventions on tidal hydrodynamics, morphology and sediment concentrations by using a hydrodynamic and sediment transport model of the Scheldt estuary in TELEMAC, while the ecological impact is studied by the University of Antwerp with their primary production model. In the IMDC study, four different disposal scenarios have been analyzed in which either the deepest parts of the navigation channel or the shallow river banks were used as disposal sites for large volumes of sand. In their Scenario 4, the most promising scenario which is also assessed in this report, the river banks in between Burcht and Rupelmonde just upstream of Antwerp (Lower Sea Scheldt) are raised to a maximum elevation of -1,0 m TAW (Figure 1), allowing for approximately 2,67 Mm^3 of sand disposal according to calculations by IMDC (2020).

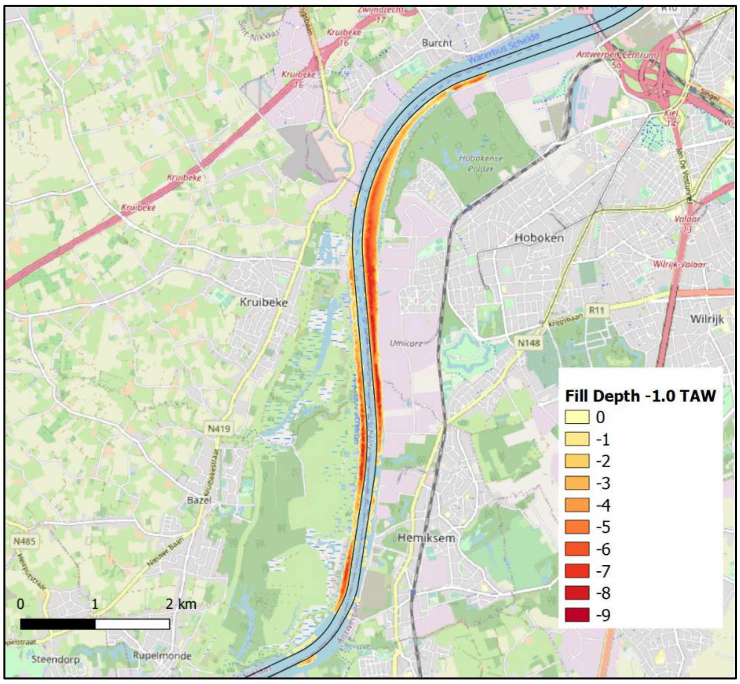

Figure 1 – Bathymetric change for IMMERSE WP3.2 Scenario 4 by IMDC (2020).

Suspended sediment concentrations along the Scheldt estuary

In addition to the positive impact of a reduced tidal range on safety, i.e., reduced high water levels, the changed hydrodynamics in Scenario 4 may also influence suspended sediment dynamics in the Scheldt estuary. In particular, suspended sediment concentrations in the Upper Sea Scheldt have been increasing gradually over the past decades (e.g. Maris & Meire, 2017). Higher sediment concentrations imply higher turbidity values and hence reduced light transmission, which on turn affect algae blooms and limit primary production (e.g. Horemans *et al.*, 2020). Therefore, the potential impact of morphological measures on SSC values in the estuary should be assessed.

Figure 2 illustrates the observed SSC variation along the estuary based on sailed half-tide-ebb measurements (Plancke *et al.,* 2020a), with a clear ETM around KM-110 to KM-140 from Vlissingen for the summer measurements, depending on the year. The observed maximum concentrations vary between 350 mg/ and 550 mg/L. The winter measurements do not contain such an ETM in the Upper Sea Scheldt. Maximum concentrations of 150-200 mg/L are then found between KM-60 and KM-100 from the estuary mouth. Differences between summer and winter conditions are mainly caused by variations in upstream river discharge (i.e., high discharge during winter and low discharge during summer) and biological factors such as algae blooms. The 2013 measurements also show a clear SSC-peak around KM-70, due to the (frequent) disposal of dredged sediment at this location. In particular, previous modelling exercises (Coen *et al.*, 2016; Stark *et al.*, in prep.) and data analyses (Plancke *et al.*, 2020b) indicate that the second SSC peak in the Lower Sea Scheldt can be attributed to disposal activities.

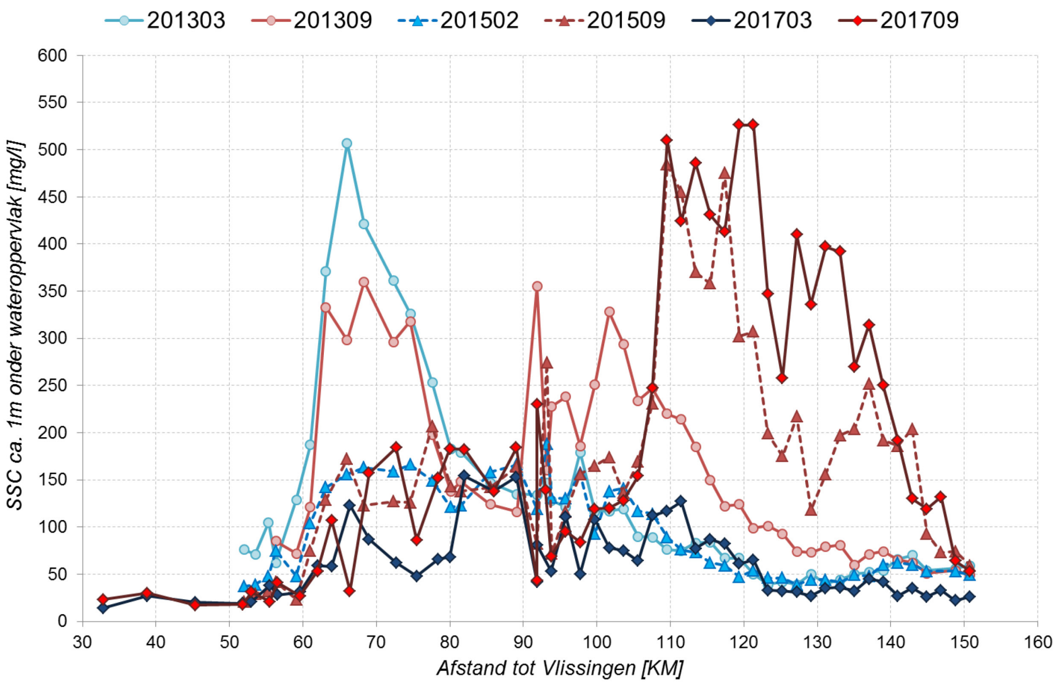

Figure 2 – Observed SSC along the Scheldt estuary based on various surface measurements. Adopted from Plancke *et al.* (2020a).

Model development in Delft3D NeVla

Recently, the Delft3D-NeVla model has been applied at Flanders Hydraulics Research by Stark *et al.* (in prep.) in order to improve the modelled representation of the observed SSC distribution over the estuary. The cohesive sediment transport model in Delft3D-NeVla is now able to represent the formation of a natural estuarine turbidity maximum (ETM) with a realistic distribution of sediment concentrations in the Upper Sea Scheldt. This modelled ETM remains present and fairly stable for simulation periods of several weeks to months (e.g. Figure 3), depending on the applied model settings and sediment characteristics. Besides, the high concentrations along a large part of the estuary at day 3 are occurring as the model redistributes sediment in an initial response of the to its initial sediment distribution.

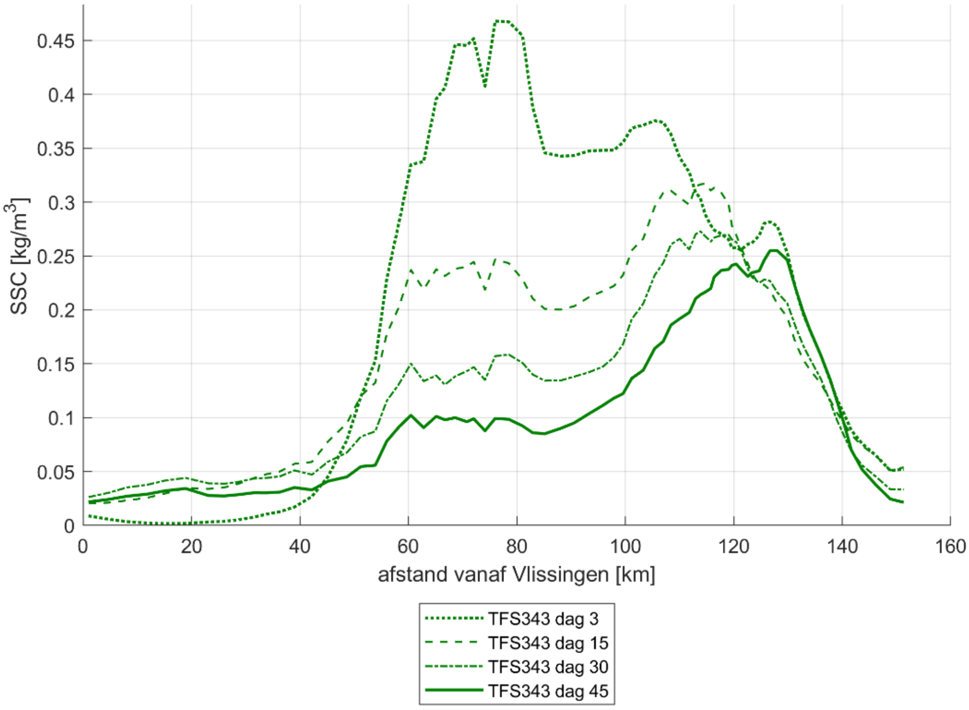

Figure 3 – Modelled tidally averaged SSC distribution along the Scheldt estuary based on a model simulation by Stark *et al.* (in prep.) for several output timesteps during the simulation.

1.2 Plan of Approach

In this report, a recently improved version of the cohesive sediment transport model in Delft3D-NeVla (Stark *et al.*, in prep.) is used to analyze the impact of the bathymetric changes in IMDC's Scenario 4 on the SSC distribution along the estuary. This impact will be investigated for a high discharge and low discharge situation. In addition, the impact of this intervention on tidal hydrodynamics is also briefly addressed.

Ultimately, the modelled impact of the proposed deposition scenario on the along-estuary distribution of SSC will be used by the University of Antwerp as input for their primary production model.

1.3 Report outline

This report consist of several sections. While the background of this study was briefly discussed in Section 1, the following sections contain the modelling setup and methodology (Section 2) and the model results (Section 3). Finally, Section 4 gives the main conclusions of this modelling exercise.

2 Model description

2.1 The Delft3D-Nevla model

The model used for this scenario analysis is the Delft3D NeVla model. This model has been used extensively to study tidal hydrodynamics and sediment transport in the Scheldt estuary. Extensive calibration and validation exercises regarding the tidal hydrodynamics in the NeVla model were carried out by Maximova *et al.* (2009) and Vanlede *et al.* (2015). In the present modeling exercise, the 2D version of the Delft3D NeVla model is applied. General information on the software itself can be found in the Delft3D-FLOW user manual (Deltares, 2016a).

Recently, Stark *et al.* (in prep.) applied the two-dimensional version of the Delft3D NeVla model to simulate suspended sediment dynamics in the Sea Scheldt. A sensitivity analysis was conducted in which the influence of various sediment characteristics, the simulation period, the upstream discharge, waves and salinity on the spatial distribution of suspended sediment and the formation of an ETM in the Upper Sea Scheldt was assessed. Moreover, Stark *et al.* (in prep.) conducted model simulations in which disposal activities were implemented in the Delft3D-NeVla model. Earlier, a refined version of the 2D NeVla sediment transport model was applied to model disposal of cohesive sediment fractions by Coen *et al.* (2016). The applied model settings for the present scenario analysis are largely adopted from those former studies.

The following sections give a brief overview of the applied model settings for the present analysis. A more detailed overview of all model settings, including settings for bottom friction and the implementation of salinity, is given by Stark *et al.* (in prep.) who specifically adapted the NeVla sediment transport model for an optimal representation of the estuarine turbidity maximum.

2.2 Settings

2.2.1 Model grid

The NeVla model grid includes the full Scheldt estuary, its tidally influenced tributaries and part of the North Sea (Figure 4). The model domain is cut off between Westkapelle and Cadzand at the estuary's mouth. By doing so, observed water level series can be used as a downstream boundary condition. The grid resolution varies between 400 m on the North Sea, 100-200 m in the Western Scheldt until an average grid cell width of approximately 30 m near Schelle. Further upstream in the Upper Sea Scheldt, the grid cell width remains similar.

It is noted that the used version of the NeVla model is adopted from the earlier study by Coen *et al.* (2016) and Stark *et al.* (in prep.) and is based on the 2011 geometry and bathymetry of the estuary. Several flood control areas that have been constructed during the last decade are therefore not included in the present model runs. Those differences between the 2011 model and the actual present situation could potentially lead to deviating tidal hydrodynamics, especially in the upstream part of the estuary. For example, the 600 ha large flood control area of Kruibeke-Bazel-Rupelmonde is not implemented in this version of the model.

Figure 4 – The original NeVla grid. White line indicates the offshore boundary used in this study

2.2.2 Bathymetric data

The applied bathymetry is adopted from an earlier modelling study on suspended sediment concentrations in the Scheldt Estuary by Coen *et al.* (2016). The bathymetry in the Western Scheldt is based on a 2011 dataset from Rijkswaterstaat. The bathymetry of the Sea Scheldt is based on 2011 measurements from Vlaamse Hydrografie. For intertidal areas, LIDAR measurements from 2011 are used.

For the present scenario analysis, the bathymetric data is adapted between Antwerp and Temse (see §2.3). Along this part of the estuary, the 2017 bathymetry is implemented based on data that was provided by the Maritime Access department of the Flemish government. It is again emphasized that the large flood control area of Kruibeke-Bazel-Rupelmonde is not included in the currently applied version of the Delft3D NeVla model.

The horizontal coordinate system is RD Parijs. The vertical reference level is m TAW.

2.2.3 Boundary conditions

Downstream boundary conditions

The downstream boundary between Westkapelle and Cadzand is forced by observed water level conditions for the period 1-1-2019 until 15-2-2019 (Figure 5). The simulation lasts 45 days. In accordance with findings by Vanlede *et al.* (2009) and Maximova *et al.* (2009), the water level time series at Cadzand is implemented with a phase shift of +10 minutes. This phase shift corrects for the 5200 m distance between the Cadzand measurement station and the downstream boundary of the model where the water level time series are implemented.

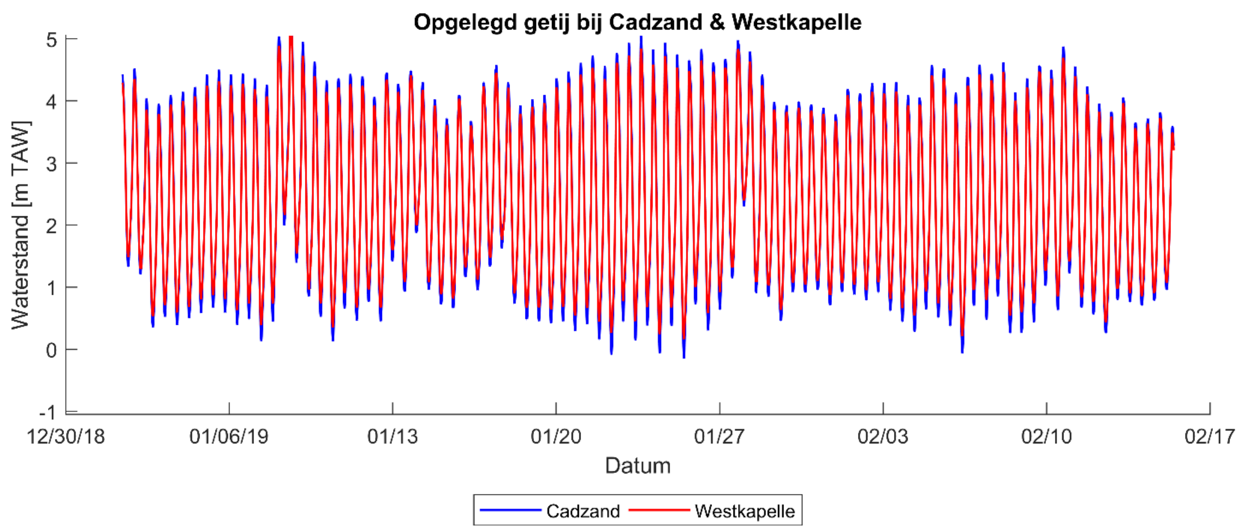

Figure 5 – Downstream water level boundary condition at Cadzand and Westkapelle.

Upstream boundary conditions

For the scenario analysis, the upstream boundaries along the Upper Sea Scheldt and tidally influenced tributaries are forced by a constant discharge. Three sets of discharge conditions are implemented: (1) a low discharge condition corresponding to the P10 values of the daily discharge measurements between 1989 and 2018; (2) a median discharge condition based on the P50 values and (3) a high discharge condition based on P90 values. Discharge data was obtained from the HIC hydrological yearbook 2019 (Vandenbruwaene *et al.*, 2020). Table 1 gives the applied discharge boundary conditions. Note that the discharges at Bath and Terneuzen are kept constant for the low and high discharge runs.

In addition, a validation run with measured daily discharge conditions for the chosen simulation period in January and February 2019 is also performed to briefly address the Delft3D NeVla version's model performance for the 2019 situation.

Table 1 – Upstream boundary conditions for low and high discharge simulations.

Boundary	Low discharge [m³/s]	Median Discharge [m³/s]	High Discharge [m³/s]	SSC [kg/m³]
Zeeschelde	4,79	22,46	88,45	0,05
Dender	1,12	3,20	13,69	0,05
Zenne	5,12	7,26	15,81	0,05
Dijle	6,15	11,18	28,12	0,05
Grote Nete	2,27	3,82	8,41	0,02
Kleine Nete	2,26	4,80	12,35	0,02
Spuikanaal Bath	10,20	10,20	10,20	0,00
Kanaal Gent-Terneuzen	31,10	31,10	31,10	0,00

Boundary conditions for sediment transport

The downstream boundary has an open boundary condition for the transport of sediment. A reference concentration of 0,03 kg/m^3 is applied here.- The upstream boundary conditions for sediment concentrations are shown in Table 1. All values were adopted from Coen *et al.* (2016).

2.2.4 Waves

Based on findings by Stark *et al.* (in prep.), the present scenario analysis is conducted with a model configuration including (wind) waves, using the Delft3D-WAVE module. In this module, the wave field is computed using a 3rd generation SWAN model (Deltares, 2016b; Booij *et al.*, 1999). The results of the Delft3D-WAVE simulation (wave height, wave period, mass transfers, bottom shear stress) are online communicated as a forcing in the Delft3D-FLOW simulation.

The wave computation is only forced by a wind forcing of 4,40 m/s (i.e., corresponding to 3 Bft), corresponding to the P50-percentile of the wind speed at Hansweert (Western Scheldt) over the 2000-2019 period. Daily wind data at an elevation of 10 m was obtained for that period from the KNMI, i.e., Netherlands Royal Meteorological Institute. The wind direction varies for each tide (i.e., north during 1^{st} tide, east during 2^{nd} tide, south during 3^{rd} tide, west during 4^{th} tide, etc.) so all wind directions occur during the model simulation. There is no external wave forcing at the downstream boundary as the area of interest is in the Sea Scheldt rather than the Western Scheldt. All waves are thus internally generated.

The impact of waves on sediment transport and sediment concentrations mainly results from additional bottom shear stress, which is most profound on shallow zones and thus enhances resuspension of sediment on tidal flats. Stark *et al.* (in prep.) also show that a model configuration with waves gives an upstream directed residual sediment load in a part of the Sea Scheldt, which could support the formation of a (stable) ETM.

2.2.5 Sediment transport

The erosion and deposition of fine (cohesive) sediment is computed by the Partheniades-Krone formula (Partheniades, 1965). The suspended sediment transport itself is computed with the formulations of Van Rijn (1993).

One single cohesive sediment fraction is used in this scenario analysis. The applied settings for the cohesive sediment fraction are summarized in Table 2. These settings were estimated based on the results of the sensitivity analyses by Stark *et al.* (in prep.) and aim at an optimal quantitative representation of the estuarine SSC variation including the ETM in the Upper Sea Scheldt.

Table 2 – Model settings for cohesive sediment.

Parameter	Value
Reference density for hindered settling calculations	c_{ref} = 1600 kg/m^3
Option for determining suspended sediment diameter	IopSus = 0 (i.e., Van Rijn, 1993 method)
Sediment type	Mud
Specific density of sediment fraction	P_{sol} = 2650 kg/m^3
Settling velocity	ω_s = 2,0 mm/s
Critical bed shear stress for sedimentation	$\tau_{kr,d}$ = 1,0 N/m^2
Critical bed shear stress for erosion	$\tau_{kr,e}$ = 0,2 N/m^2
Erosion Parameter	M_E = 2,0·10^{-3} kg/m^2/s
Dry bed density	CDryB = 550 kg/m^3

Sediment availability

The variable initial thickness of the sediment layer shown in Figure 6 results from a previous model simulation of 45 days. More details on this initial run and the distribution of the sediment layer thickness is given in Stark *et al.* (in prep.). Most sediment is situated in sheltered zones along the estuary, such as tidal docks and intertidal areas. The availability of sediment on the bottom of the estuary channel on the other hand is small.

Besides, the initial layer thickness in the Western Scheldt is set to 0 m as test runs in the sensitivity analysis by Stark *et al.* (in prep.) give unrealistic or erroneous results if sediment is implemented in the vicinity of the downstream boundary between Cadzand and Westkapelle.

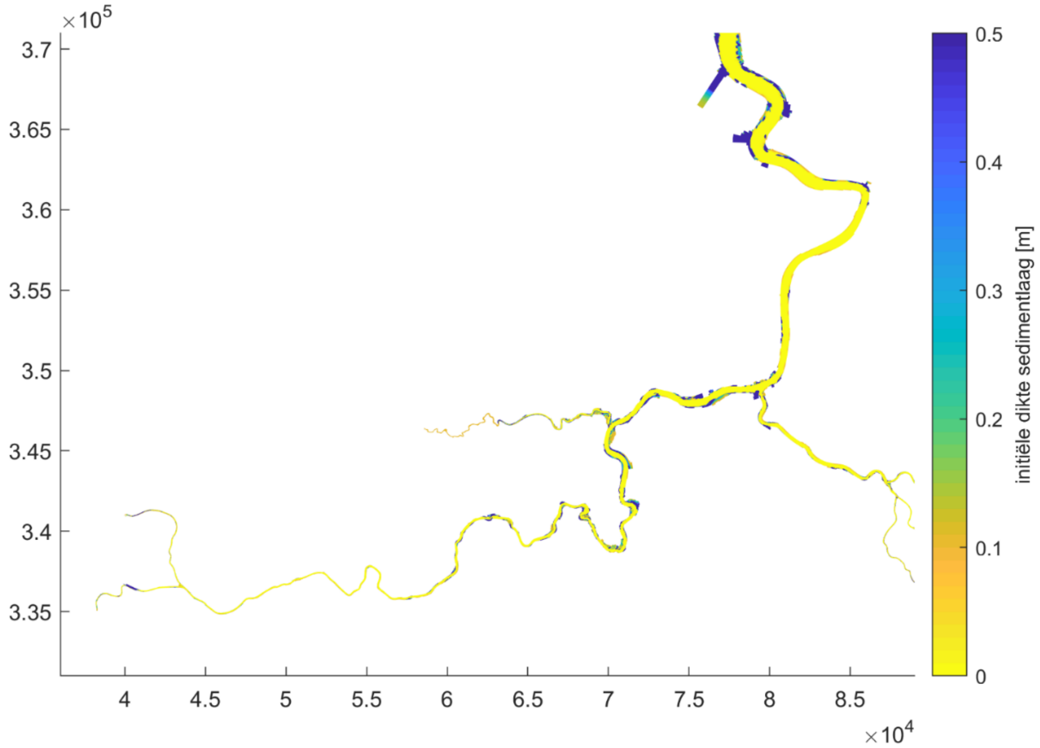

Figure 6 – Initial sediment layer thickness in the Sea Scheldt.

2.3 Implementation of Scenario 4

In IMMERSE WP3.2 Scenario 4, developed by IMDC (2020), the bed level on both river banks is raised until an elevation of -1,0 m TAW over a section between Burcht and Rupelmonde (Figure 7). This bathymetric adaptation corresponds to a volume of 2,67 Mm^3 of disposed sand (IMDC, 2020).

The sand disposal scenario is implemented by a bathymetric adaptation of the bottom level. No actual sediment is added to the model. Applying a fixed bed does assure a representative morphology throughout the simulation. This methodology assumes that the disposed sediment remains stable over time and therefore does not account for morphological changes that could be initiated by the intervention.

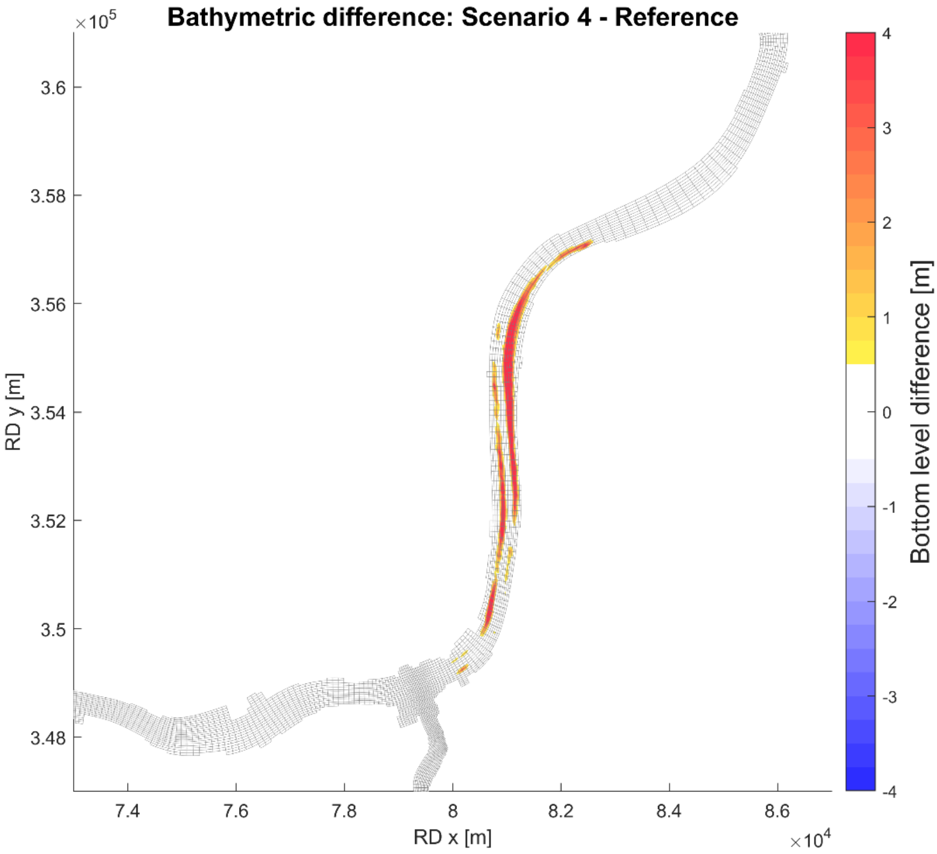

Figure 7 – Bathymetric difference between Scenario 4 and the reference scenario.

3 Results

3.1 Tidal hydrodynamics

3.1.1 Model validation of vertical tide based on reference run

Appendix A – Model validation for vertical tide contains a comparison between modelled and observed tidal water levels along the estuary based on the reference run. The model performance of the reference run is assessed by the RMSE and BIAS values that are computed relative to observed water level time series. The RMSE and BIAS based on the full water level time series are given in Figure 19 and Figure 20 respectively. The BIAS of the modelled high and low water levels and phases specifically are included in Figure 21 (ΔHW), Figure 22 (ΔT_{HW}), Figure 23 (ΔLW) and Figure 24 (ΔT_{LW}). In addition, the modelled and observed M2, M4 and M6 tidal components are compared in Figure 25 – Figure 30.

The overall representation of the tidal wave is fairly good with RMSE values of < 0,15 m in the Western Scheldt and Lower Sea Scheldt and somewhat higher RMSE values of approx. 0,25 m in the most upstream part of the Upper Sea Scheldt. Similarly, the overall BIAS of the water level time series is generally < 0,02 m for tidal stations up until StAmands. Further upstream, the BIAS is larger with a maximum deviation of -0,12 m at Melle.

If the high water level BIAS and low water level BIAS are considered, the model performance is again good in the Western Scheldt and Lower Sea Scheldt with deviations < 0,05 m. However, the deviation between the modelled and observed high- and low water levels gradually increases towards the upstream part of the Upper Sea Scheldt. High water levels are overestimated by +0,11 m at Temse up to +0,23 m at Melle, whereas low water levels are underestimated by -0,18 m at Temse up until -0,50 m at Melle. This implies an overestimation of the tidal range in the Upper Sea Scheldt. The overestimation of the tidal range also follows from the M2 amplitude comparison in Figure 25, which clearly shows an increased tidal penetration in the simulation compared to the observations. The model's overestimation of tidal penetration (i.e., tidal range, tidal wave celerity and M2 amplitude) in the most upstream part of the estuary can partly be explained by the choice for the version of the Delft3D-NeVla model grid with a 2011 bathymetry and without some recently implemented flood control areas (e.g. Kruibeke-Bazel-Rupelmonde, Bergenmeersen). Other possible causes for these deviations in the Upper Sea Scheldt could be the grid cell resolution and the bottom friction-field, which was also calibrated for 2011. The high and low water phase, related to the celerity of the high and low water along the estuary, are well represented by the model with a ΔT_{HW} of +0 up to +8 minutes and a ΔT_{LW} of -6 up to +8 minutes in most part of the estuary, except for the most upstream tidal stations at Wetteren and Melle, where the modelled low waters occur 10-15 minutes earlier than in the observations.

The comparison of the modelled and observed M4 amplitudes in Figure 27 shows that the model slightly underestimates the M4 tide along the estuary. This underestimation is limited to -0,01 m in the Western Scheldt, but increases to about -0,05 m in the Sea Scheldt. As for the deviation of the M2 amplitude, the use of an older bathymetry and geometry in the model is likely causing the underestimation of M4 in the upstream part of the estuary. In particular, the presence of intertidal areas is known to transfer energy from the M2 constituent to its M4 overtide (e.g. Friedrichs & Aubrey, 1988). The M6 tide is well represented with deviations of less than 0,01 m along the estuary. Besides, the modelled and observed phase of the M2, M4 and M6 constituents correspond fairly well.

Finally, the modelled and observed M4/M2 amplitude ratios (Figure 31) and the 2M2-M4 phase differences (Figure 32) are also compared for tidal stations along the estuary. The 2M2-M4 phase difference between the M2 constituent and the M4 overtide is considered representative for phase differences between other semi-diurnal and quarter-diurnal constituents (e.g. Friedrichs & Aubrey, 1988) and can be used to indicate the nature of the asymmetry of the tidal signal (i.e., whether the tide is flood-dominant or ebb-dominant). If the M2 and M4 constituents of the vertical tide are considered, phase differences between 0° < 2M2-M4 < 180° indicate that the vertical tidal asymmetry tends to be flood dominant with a shorter water level rise than fall, whereas a phase difference between -180° < 2M2-M4 < 0° indicates an ebb-dominant asymmetry with a longer water level rise. The observed and modelled 2M2-M4 phase differences gradually increase along the estuary with values close to 0° in the Western Scheldt and values up to 70° (flood-dominant) in the Upper Sea Scheldt. The model slightly overestimates the rate of this flood-dominant asymmetry in the Lower Sea Scheldt based on the tidal component analysis. Furthermore, amplitude ratios between the M4 overtide and the M2 principal tidal constituent are indicators for the strength of the tidal asymmetry. Higher amplitude ratios imply a stronger tidal asymmetry, while lower ratios indicate more symmetric tides. These ratios are underestimated by a few percent in the Sea Scheldt, which could be expected given the overestimation of M2 and the underestimation of M4 in the upstream part of the estuary. As stated before, the underestimation of the tidal asymmetry can partly be explained by the absence of certain intertidal areas, as well as by the use of an older bathymetry.

In conclusion, the model performance regarding the representation of the vertical tide is considered good in the Western Scheldt and Lower Sea Scheldt, although the strength of the tidal asymmetry is underestimated from Bath upwards. In the Upper Sea Scheldt however, the tidal penetration is overestimated for the 2019 conditions. To avoid a large influence of the deviations that are present for the 2019 tidal conditions, the different scenarios will be analyzed relative to each other.

3.1.2 Impact on tidal hydrodynamics in Scenario 4

The impact of Scenario 4 on vertical tidal hydrodynamics is here briefly assessed by looking into the changes in high- and low water levels and in the M2 and M4 tidal components. The hydrodynamic impact is analyzed for the median discharge scenarios. A more detailed impact analysis on tidal hydrodynamics, including the scenario's influence on tidal velocities and salinity, was provided by IMDC (2020).

While the impact of the bathymetric scenario on high and low water levels resembles the effect on tidal penetration and tidal range, the change in the 2M2-M4 phase difference and M4/M2 amplitude ratio can be used as proxy for the scenario's influence on tidal asymmetry. Figure 8 and Figure 9 show the impact of the bathymetric change in Scenario 4 on tidal hydrodynamics based on the high and low water levels respectively. The impact is computed as a "BIAS", meaning the difference between scenario 4 and the reference scenario. In addition, Figure 10 and Figure 11 illustrate the impact of Scenario 4 on tidal asymmetry based on the 2M2-M4 phase difference and M4/M2 amplitude ratio. These figures are based on the results of the median discharge runs.

According to the Delft3D model analysis, the implementation of Scenario 4 leads to a reduction in tidal range in the Upper Sea Scheldt, ranging from -0,13 m in Temse to -0,04 m in Melle. The impact on high waters is stronger at Temse (-0,08 m), but decreases in an upstream direction. The impact on low waters is quite similar for all upstream tidal stations (i.e., -0,04 to -0,03 m). In contrast to the upstream impact, the tidal range slightly increases by 0,01-0,02 m downstream and along the altered section between Burcht and Rupelmonde (i.e., at Liefkenshoek and Antwerpen). Overall, the strongest impact is thus found directly upstream of the bathymetric adaptations. The influence on high- and lower water levels is almost similar for the high- and low discharge scenarios.

The scenario's influence on vertical tidal asymmetry is quite small based on the harmonic component analysis. According to the 2M2-M4 phase difference, the shape of the tidal wave becomes slightly more flood dominant from KM-100 onwards, i.e., upstream of the bathymetric changes. Conversely, the shape of the tidal wave becomes a bit less flood-dominant downstream and along the altered section. The strength of the tidal asymmetry slightly increases along and upstream of the Burcht-Rupelmonde section.

For the high discharge runs, the hydrodynamic impact of Scenario 4 on the M2 and M4 tide is almost identical as for low discharge conditions (not shown in figures). The high discharge itself does however alter the tidal components in the upstream part of the estuary. In those runs, the M2 amplitude is up to 0,20 m lower in the most upstream part of the estuary, while the M2 and M4 phases are shifted by up to -2° and -6° respectively in the Upper Sea Scheldt.

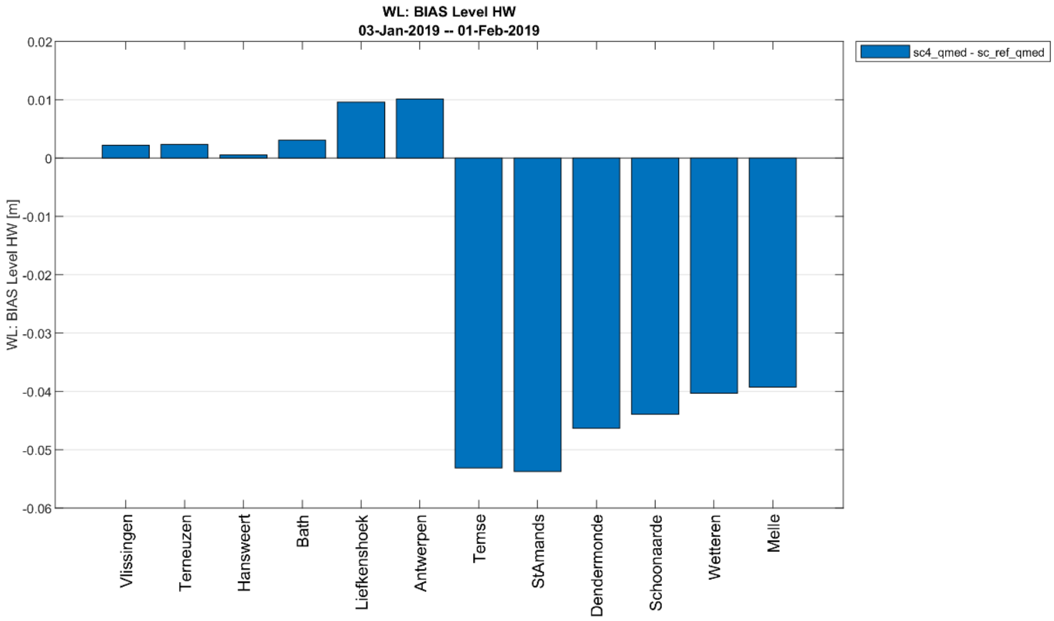

Figure 8 – Impact on high water levels in Scenario 4.

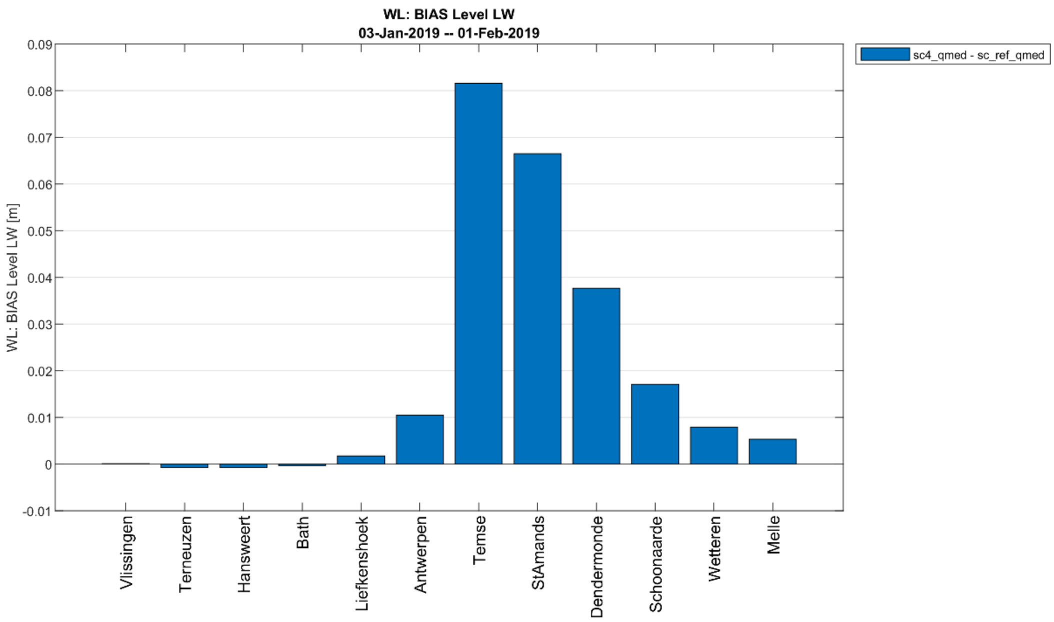

Figure 9 – Impact on low water levels in Scenario 4.

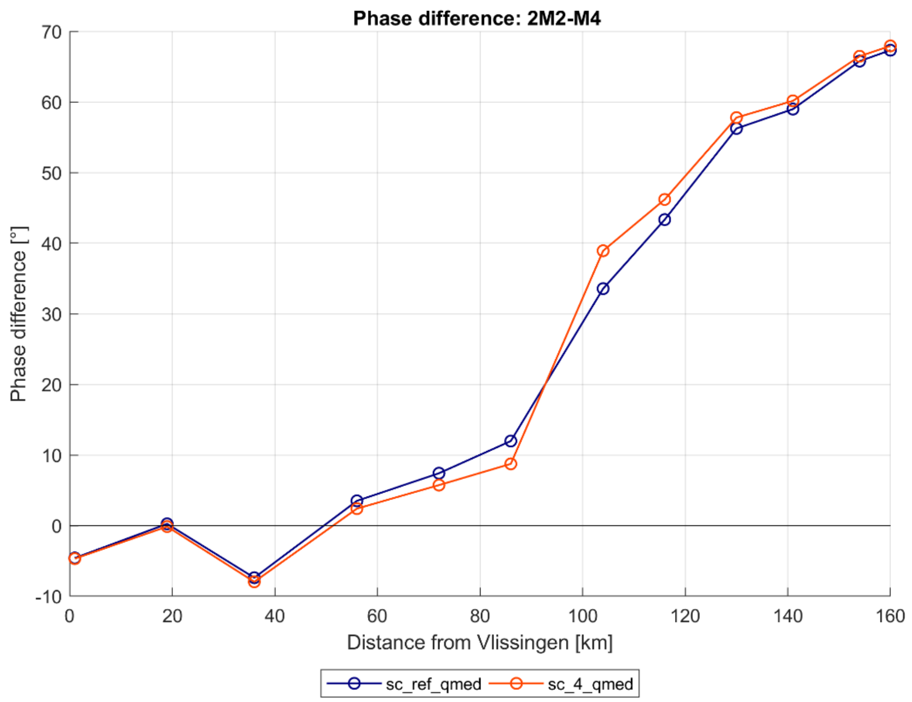

Figure 10 – 2M2-M4 phase difference in model scenarios.

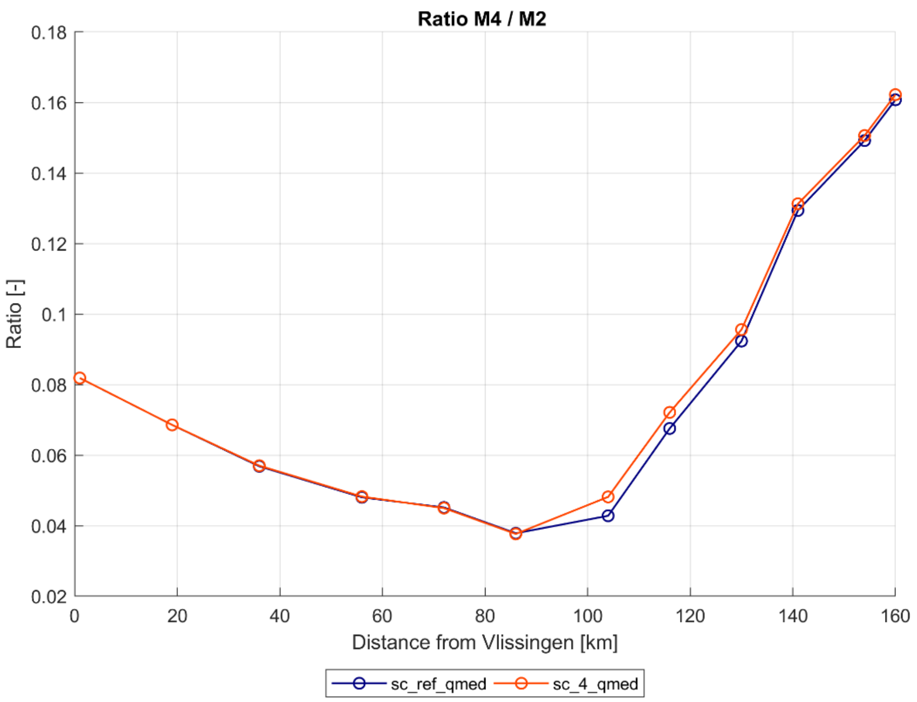

Figure 11 – M4/M2 amplitude ratio in model scenarios.

3.2 SSC

3.2.1 SSC variation in reference run

Figure 12 shows the modelled along-estuary distribution of SSC for three spring-neap cycles in the reference run with low discharge. Figure 13 gives the spring-neap averaged (i.e., 3rd spring-neap-cycle) spatial SSC variation for the reference run (in black). The modelled spatial variation corresponds well with the observations shown in Figure 2. That is, the modelled ETM near KM-120 is also present in the measured distribution for summer, although the modelled ETM is situated a few kilometers more upstream. The height of the SSC-peak of approx. 400-500 mg/L over the last two spring-neap cycles also corresponds to the height of the measured peak in this region (Figure 2). The observed peak in the Lower Sea Scheldt, i.e., near KM-70, is not present in the model. However, this SSC-peak is likely caused by sediment disposal in this region. Such dredging and disposal activities are not implemented in the present model simulations. Stark *et al.* (in prep.) do show that this SSC-peak may also be reproduced if disposal activities are implemented. The development over time indicates a decrease and upward shift of the SSC-peak. Nevertheless, the modelled ETM is persistent for the 1,5 month duration of the model simulation. Sediment concentrations are however decreasing continuously downstream of the ETM in the Lower Sea Scheldt. Stark *et al.* (in prep.) attributed this decrease to the net downstream residual transport and the loss of sediment in sheltered zones, such as tidal docks or tidal flats.

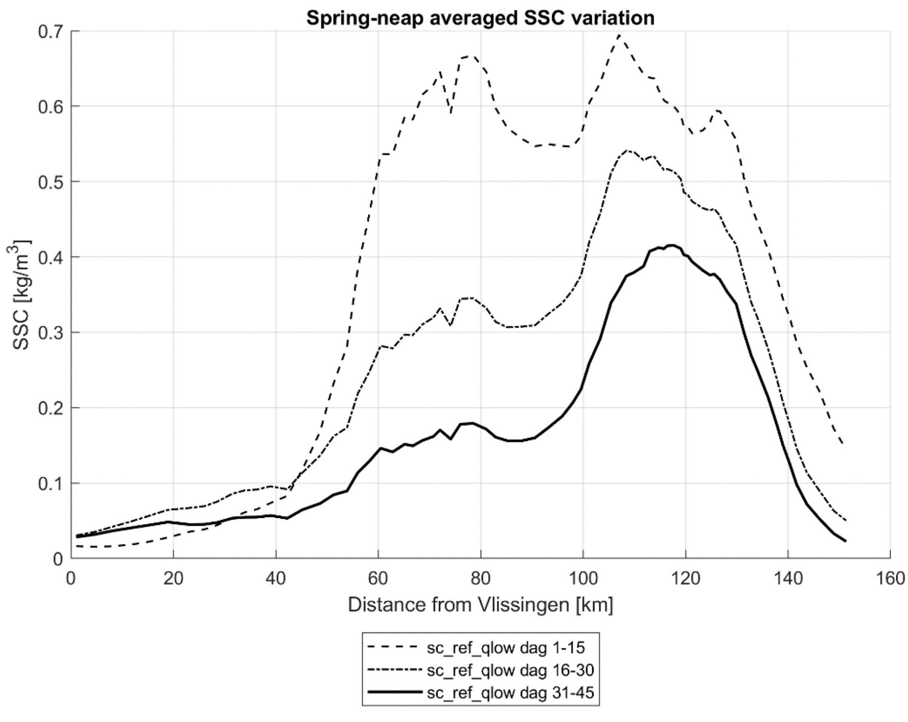

Figure 12 – Along estuary SSC-variation for the reference situation with low discharge conditions.

3.2.2 Impact on SSC in Scenario 4

Figure 13 shows the spring neap averaged SSC distribution over the last spring-neap cycles in the reference scenario and Scenario 4 with low discharge conditions. Figure 14 depicts the relative impact of the bathymetric changes in Scenario 4 on the spatial SSC distribution along the estuary in a low discharge situation. The bathymetrical changes in Scenario 4 lead to a small SSC decrease in the Lower Sea Scheldt and a SSC increase from KM-110 onwards in the Upper Sea Scheldt. The maximum spring-neap-averaged SSC values at the ETM increase from a maximum of about 420 mg/L to 480 mg/L in Scenario 4. This implies an increase of 15% of the maximum sediment concentrations in the estuary. Locally, stronger SSC increases of up to +40% at KM-130 are modelled. The relative SSC decrease in the Lower Sea Scheldt is much less (i.e., up to -10%), while the impact on SSC in the Western Scheldt is negligible.

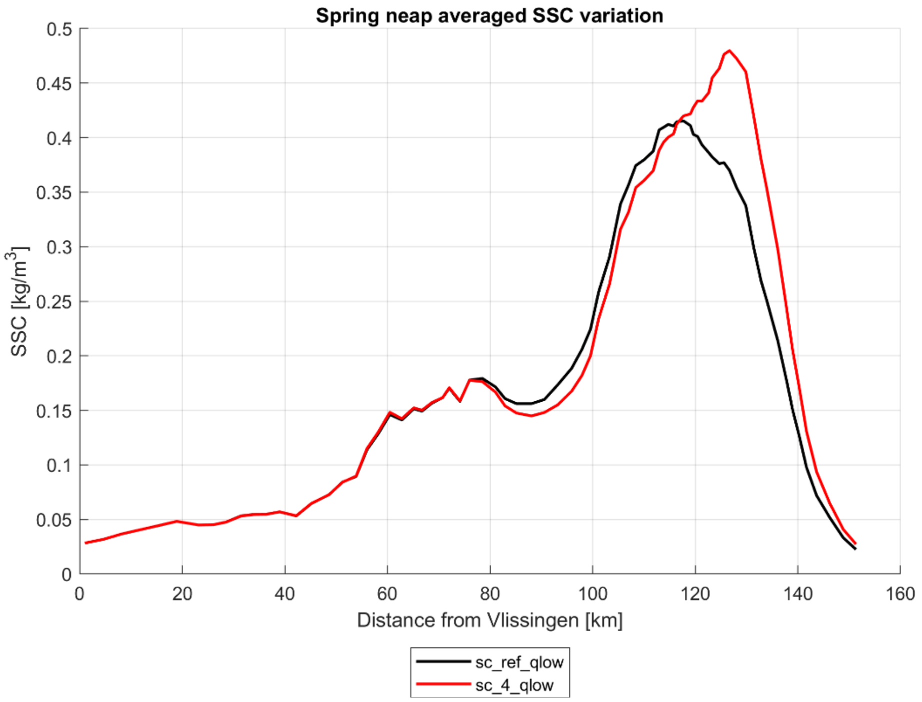

Figure 13 – Along estuary SSC-variation averaged over one spring-neap cycle for between Scenario 4 and the reference situation.

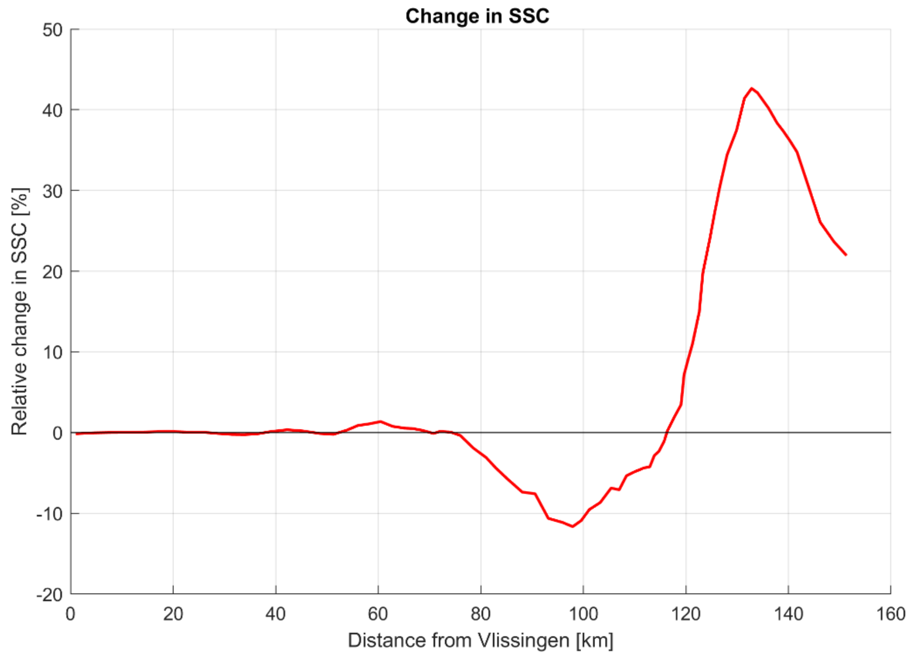

Figure 14 – Relative change in along estuary SSC variation between Scenario 4 and the reference situation.

3.2.3 Low discharge vs. high discharge

Reference situation

Firstly, Figure 15 shows the spring-neap averaged SSC distribution for the low, median and high discharge runs in the reference situation for the 3rd spring-neap cycle in the simulations. Figure 16 depicts the relative difference between these spring-neap averaged SSC for the high and low discharge runs compared to the median discharge run for the reference scenario.

From these figures, it follows that low discharge conditions lead to a strong SSC increase between KM-110 and the upward estuarine boundary, corresponding with an upward shift of the ETM. High discharges on the other hand lead to a SSC reduction in the zone in which the ETM is situated (i.e., KM-110 until KM-140) and hence a downstream shift of the ETM. Downstream of this zone, in the Western Scheldt and part of the Lower Sea Scheldt, SSC values increase as sediment from the ETM is probably washed away in a downstream direction. Besides, the high discharge condition also leads to a slight increase in SSC near the upstream boundary, potentially related to a higher sediment input from upstream.

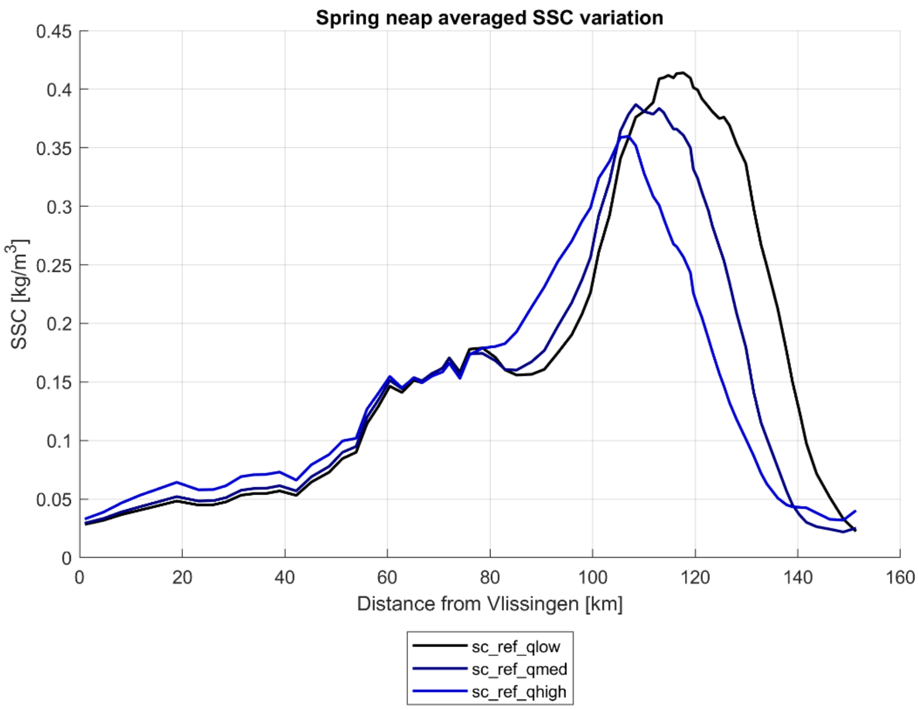

Figure 15 – Along estuary SSC variation for low and high discharge runs.

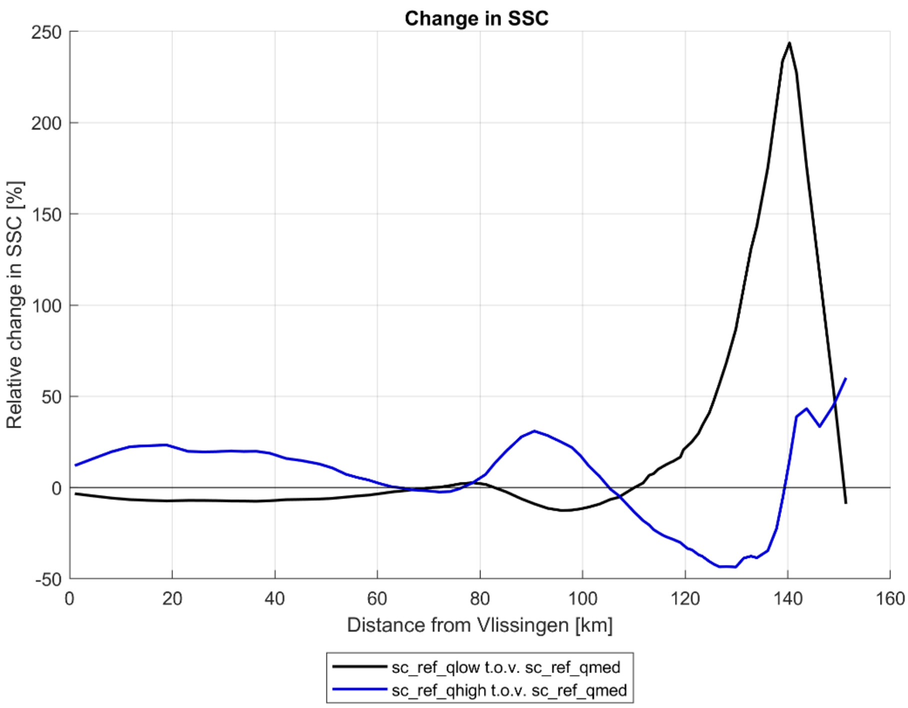

Figure 16 – Relative change in SSC for high and low discharge runs compared to median discharge run for reference situation.

Scenario 4

Figure 17 shows the spring neap averaged SSC distribution for the high – and low discharge runs of the reference scenario and Scenario 4. In addition, Figure 18 depicts the impact of the bathymetric changes in Scenario 4 on the SSC distribution in a high discharge situation. The relative impact of Scenario 4 for a low discharge situation was shown earlier in Figure 14.

During high discharge conditions, the along-estuary variation in SSC is fairly similar for Scenario 4 and the reference run. Hence, the impact of the bathymetrical changes in Scenario 4 on SSC is much smaller for high discharge conditions than for low discharge conditions. In particular, SSC values only decrease by up to -6% in the Lower Sea Scheldt and increase by up to +8% in the Upper Sea Scheldt. In conclusion, the change in SSC distribution is dominated by the hydrodynamic impact of the increased upstream discharge, rather than by the hydrodynamic impact of Scenario 4.

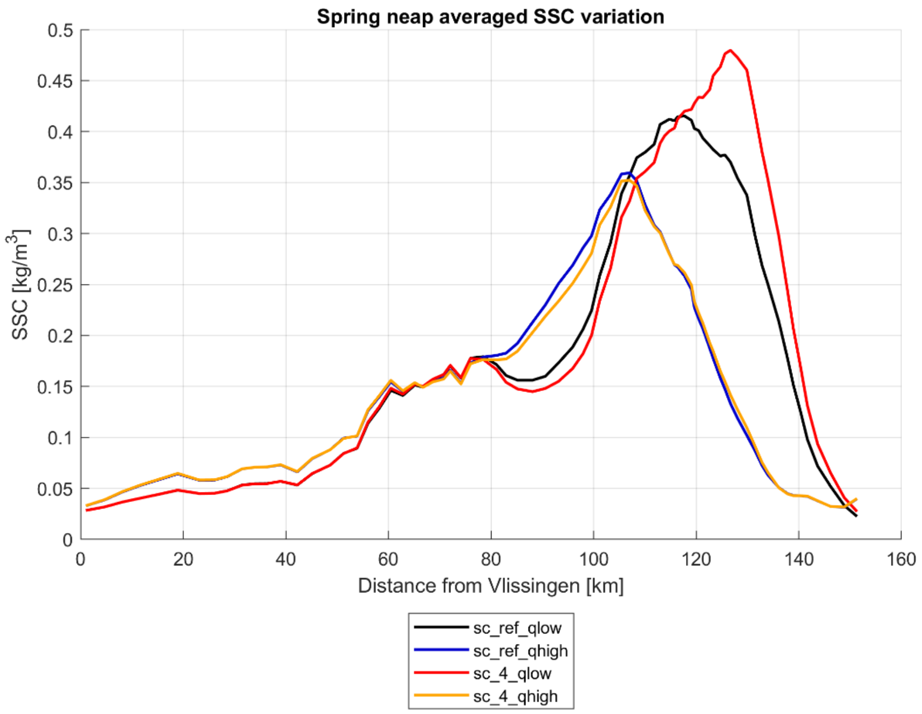

Figure 17 – Along estuary SSC variation for low and high discharge runs in Scenario 4 and the reference situation.

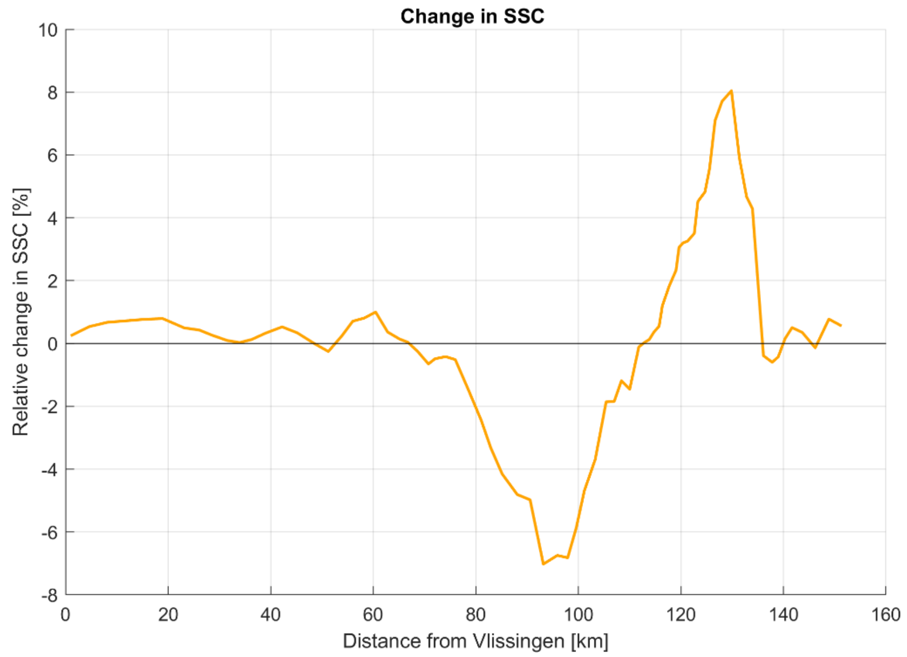

Figure 18 – Relative change in along estuary SSC variation between Scenario 4 and the reference situation for high discharge runs.

4 Conclusions

In the context of the Interreg project IMMERSE, Flanders Hydraulics Research was asked to apply a recently improved version of the cohesive sediment transport model in Delft3D-NeVla (Stark *et al.*, in prep.) to analyze the impact of the bathymetric changes in the so-called Scenario 4 by IMDC (2020) on the SSC distribution along the estuary. In this Scenario 4, the river banks in between Burcht and Rupelmonde (Lower Sea Scheldt) are raised to a maximum elevation of -1,0 m TAW, allowing for approximately 2,67 Mm^3 of sand disposal according to calculations by IMDC (2020). Ultimately, the obtained along-estuary distribution of SSC can be used as input for an ecological primary production model by the University of Antwerp.

Based on the Delft3D-NeVla simulations, these bathymetric changes lead to a tidal range reduction of up to -0,13 m at Temse. In addition, the shape of the tidal wave becomes slightly more flood dominant upstream of the bathymetric changes and a bit less flood-dominant along and downstream of the altered section. These findings correspond qualitatively to the conclusions in IMDC (2020), although they predict a stronger influence on tidal range of up to -0,25 m.

Additionally, the bathymetric changes in Scenario 4 lead to a SSC reduction of up to 10% in the Lower Sea Scheldt and a SSC increase of 10-40% in the Upper Sea Scheldt for a low discharge situation. This implies an upward movement of the ETM of about 10-15 km. The impact during high discharge conditions is much smaller (i.e., SSC reduction of up to 6% in the Lower Sea Scheldt and SSC increase of up to 8% in the Upper Sea Scheldt). In particular, the modelled spatial SSC variation hardly differs between Scenario 4 and the reference scenario for high discharge runs. The estuarine stretches over which SSC increases or decreases in Scenario 4 correspond fairly well with the zones in which the tidal asymmetry becomes more or less flood-dominant. Besides, the above results do not necessarily apply to SSC peaks as a result of disposal activities in the Lower Sea Scheldt.

The modelled spatial impact on SSC differs strongly from the modeling exercise by IMDC (2020), who model the strongest impact of Scenario 4 along and downstream of the altered section between Burcht and Rupelmonde. However, their modelled reference situation contains an ETM which is situated near Oosterweel in the Lower Sea Scheldt, far downstream of the observed natural ETM in the Upper Sea Scheldt. The latter is better represented in the current model analysis. Previous modelling studies (Coen *et al.*, 2016; Stark *et al.*, in prep.) and data analyses (Plancke *et al.*, 2020b) indicate that the ETM in the Lower Sea Scheldt is a temporal phenomenon that is induced by disposal activities. Therefore, the influence of the bathymetric changes in Scenario 4 on the downstream ETM in the Lower Sea Scheldt should be studied in a modeling exercise that includes these disposal activities.

Finally, it should be stated that this assessment was carried out based on the assumption that the implemented bathymetric changes remain stable. In reality, large scale disposal of sand and the consequent changes in tidal hydrodynamics may on its turn induce morphological changes in the estuary. Such morphodynamic feedback mechanisms may reduce the initial impact on tidal hydrodynamics and hence alter the impact on along-estuary SSC distribution. Moreover, the model assessment by IMDC (2020) indicates that bed shear stresses on the river banks increase significantly at the sites where sand is disposed and that the disposed sand on the banks would be rather unstable.

5 References

Booij, N., Ris, R.C., Holthuijsen, L.H. (1999). A third-generation wave model for coastal regions. Part 1: Model description and validation. *Journal of Geophysical Research*, 104 (C4), 7649-7666.

Coen, L.; De Maerschalck, B.; Plancke, Y.; Verwaest, T.; Mostaert, F. (2016). Sedimentstrategie Beneden-Zeeschelde: Deelrapport 1 – Opzet en validatie van het numerieke model voor het modelleren van slib. Versie 4.0. *WL Rapporten*, 14_025. Waterbouwkundig Laboratorium: Antwerpen, België.

Deltares (2016a). Delft3D-FLOW - Simulation of multi-dimensional hydrodynamic flows and transport phenomena, including sediments - User Manual. Version 3.15, Revision 49020. Delft, Nederland.

Deltares (2016b). Delft3D-Wave – Simulation of short-crested waves with SWAN - User Manual. Version 3.05, Revision 49030. Delft, Nederland.

Friedrichs, C.T.; Aubrey, D.G. (1988). Non-linear Tidal Distortion in Shallow Well-Mixed Estuaries: a Synthesis. *Estuar. Coast. Shelf Sci*. 27, 521–545. doi:10.1016/0272-7714(90)90054-U

Horemans, D. M.; Meire, P.; Cox, T. J. (2020). The impact of temporal variability in light-climate on time-averaged primary production and a phytoplankton bloom in a well-mixed estuary. *Ecological Modelling*, 436, 109287.

IMDC (2020). IMMERSE – Modelling study on sediment management of estuaries. Final Report. Version 2.0. I/RA/11579/20.081/TWO/.

Maris, T.; Meire, P. (2017). Onderzoek naar de gevolgen van het Sigmaplan, baggeractiviteiten en havenuitbreiding in de Zeeschelde op het milieu. Geïntegreerd eindverslag van het onderzoek verricht in 2016. 158 pp.

Maximova, T.; Ides, S.; De Mulder, T.; Mostaert, F. (2009). LTV O&M thema Veiligheid - Deelproject 1: Verbetering hydrodynamisch NeVla model ten behoeve van scenario-analyse. *WL Rapporten*, 756_05. Flanders Hydraulics Research & Deltares: Antwerpen, België.

Partheniades, E. (1965). Erosion and Deposition of Cohesive Soils. *Journal of the Hydraulics Division*, ASCE 91 (HY 1): 105-139.

Plancke, Y.; Mostaert, F. (2020a). AvdT – Sedimenttransport op verschillende tijdschalen: Deelrapport 1 – Slibtransport in het Schelde-estuarium. Versie 1.0. *WL Rapporten*, 17_088_1. Waterbouwkundig Laboratorium: Antwerpen, België.

Plancke, Y.; Smolders, S.; Mostaert, F. (2020b). Agenda v/d Toekomst – Sedimenttransport op verschillende tijdschalen: Deelrapport 14 – Data-analyse met behulp van een multivariaat model naar invloedsfactoren op de sedimentconcentratie in de Zeeschelde. Versie 3.0. *WL Rapporten*, 17_088_14. Waterbouwkundig Laboratorium: Antwerpen.

Stark, J.; Smolders, S.; Plancke, Y.; Mostaert, F. (in prep.). AvdT – Sedimenttransport op verschillende tijdschalen: Deelrapport 23 – Gevoeligheidsanalyse Delft3D slibmodel. Versie 1.0. *WL Rapporten*, 17_088_23. Waterbouwkundig Laboratorium: Antwerpen, België.

Stark, J.; Plancke, Y.; Mostaert, F. (in prep.). AvdT – Sedimenttransport op verschillende tijdschalen: Deelrapport 24 – Stortscenario's met Delft3D slibmodel. Versie 1.0. *WL Rapporten*, 17_088_24. Waterbouwkundig Laboratorium: Antwerpen, België.

Van Rijn, L. (1993). Principles of Sediment Transport in Rivers, Estuaries and Coastal Seas. Aqua Publications, 386 pp.

Vandenbruwaene, W.; Michielsen, S.; Hertoghs, R.; Boeckx, L.; Vereecken, H.; Deschamps, M.; Mostaert, F. (2020). Hydrologie bevaarbare waterlopen in Vlaanderen: Jaar 2019. Versie 4.0. *WL Rapporten*, PA026_3. Waterbouwkundig Laboratorium: Antwerpen.

Vanlede, J.; De Clercq, B.; Decrop, B.; Ides, S.; van Holland, G.; De Mulder, T.; Mostaert, F. (2009) Permanente verbetering modelinstrumentarium. Verbetering Randvoorwaardenmodel. Deelrapport 2: Afregeling van het 2D Scheldemodel. Waterbouwkundig Laboratorium en IMDC (I/RA/11313/09.012/BOB), Antwerpen, België.

Vanlede, J.; Delecluyse, K.; Primo, B.; Verheyen, B.; Leyssen, G.; Plancke, Y.; Verwaest, T.; Mostaert, F. (2015). Verbetering randvoorwaardenmodel: Subreport 7 - Calibration of NEVLA 3D. Version 4.0. *WL Rapporten*, 00_018. Flanders Hydraulics Research & IMDC: Antwerp, Belgium.

Appendix A – Model validation for vertical tide

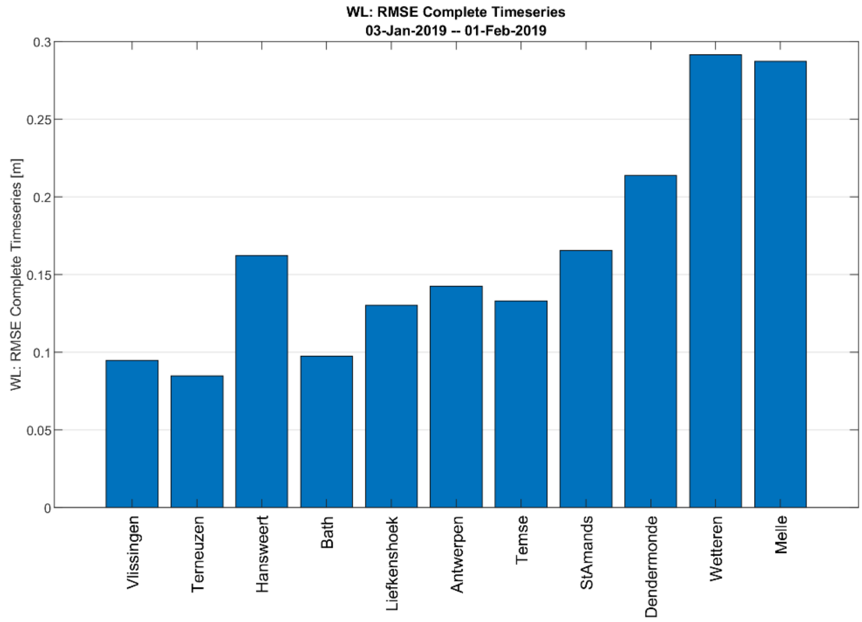

Figure 19 – RMSE on complete water level time series in validation run.

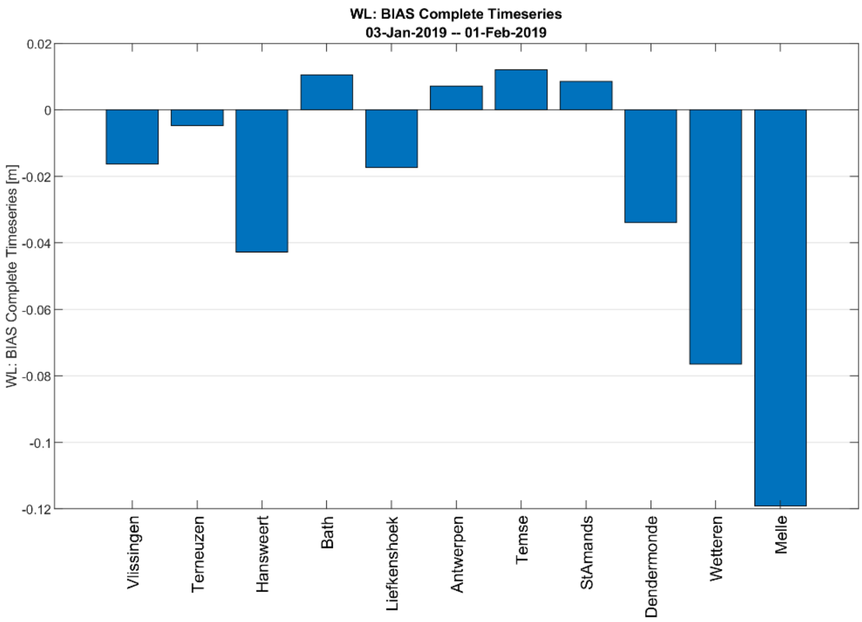

Figure 20 – BIAS of complete water level time series in validation run.

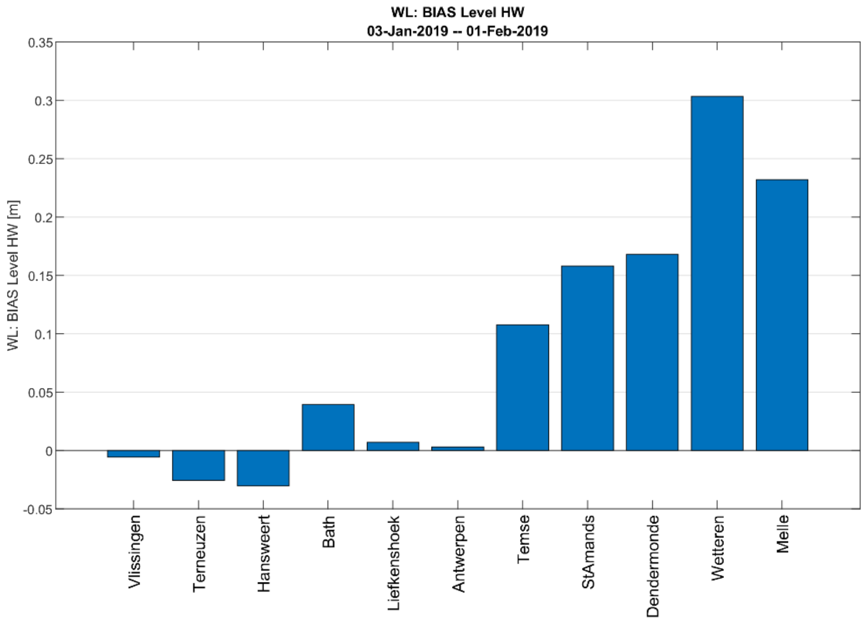

Figure 21 – BIAS of high water levels in validation run.

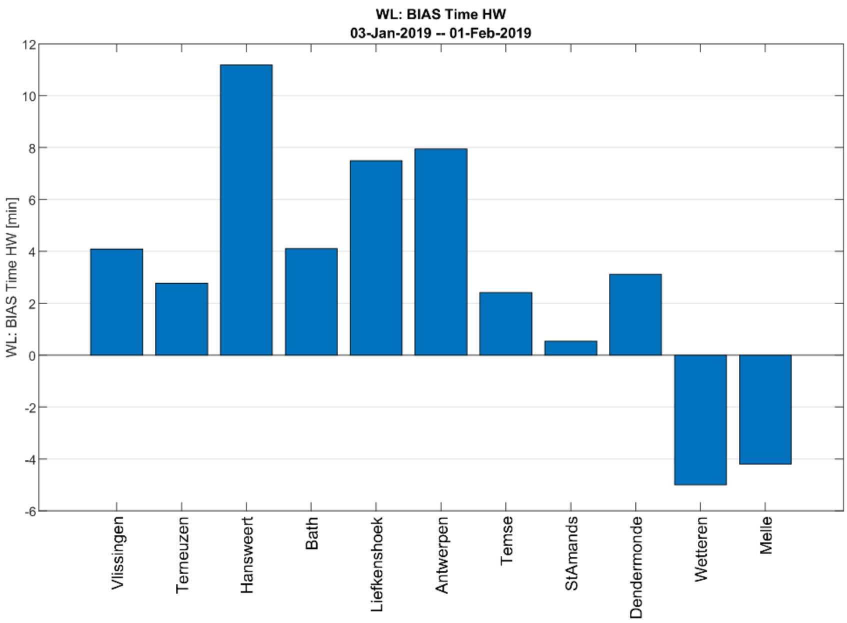

Figure 22 – BIAS of high water level phase in validation run.

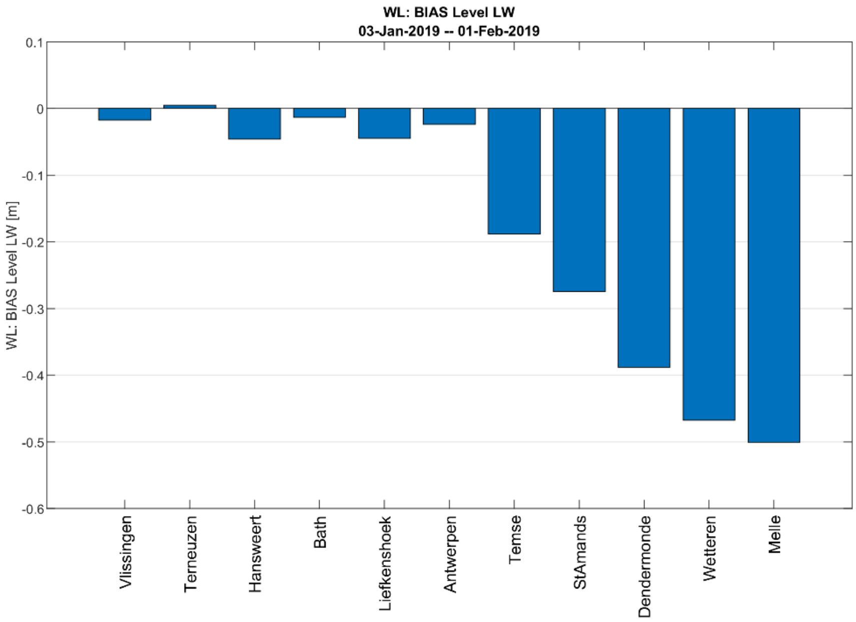

Figure 23 – BIAS of low water levels in validation run.

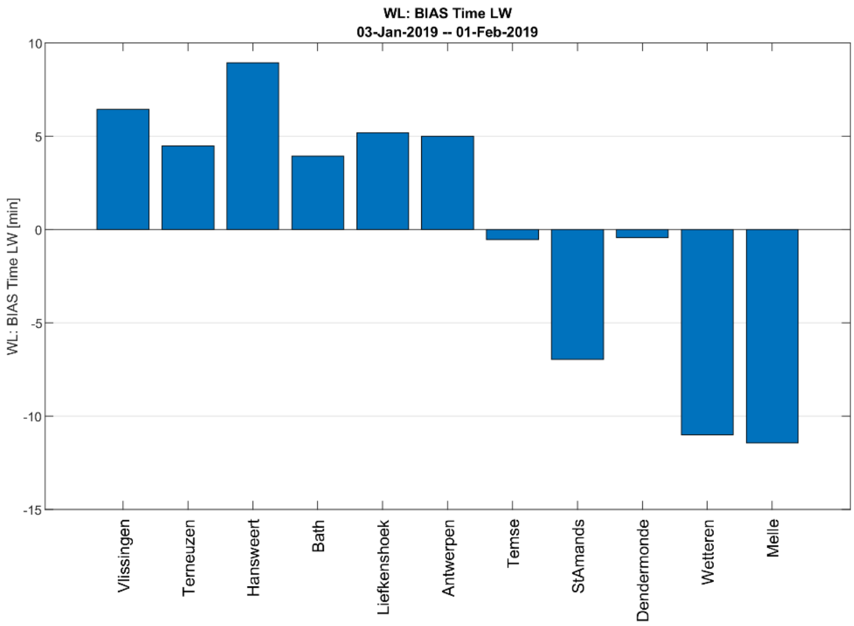

Figure 24 – BIAS of low water level phase in validation run.

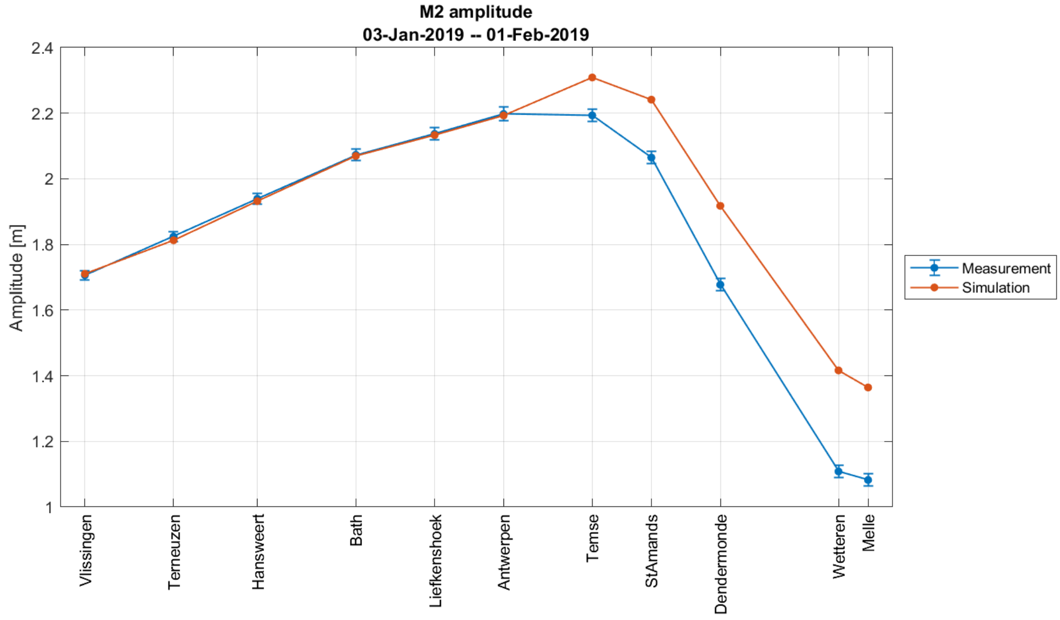

Figure 25 – Comparison between observed and modelled M2 amplitude for the validation run.

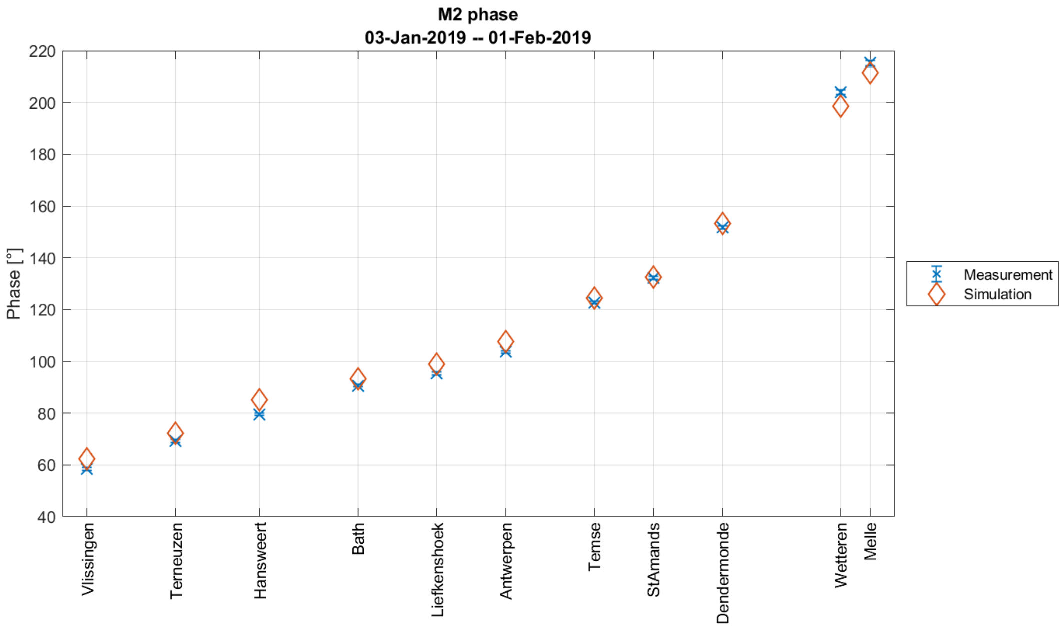

Figure 26 – Comparison between observed and modelled M2 phase for the validation run.

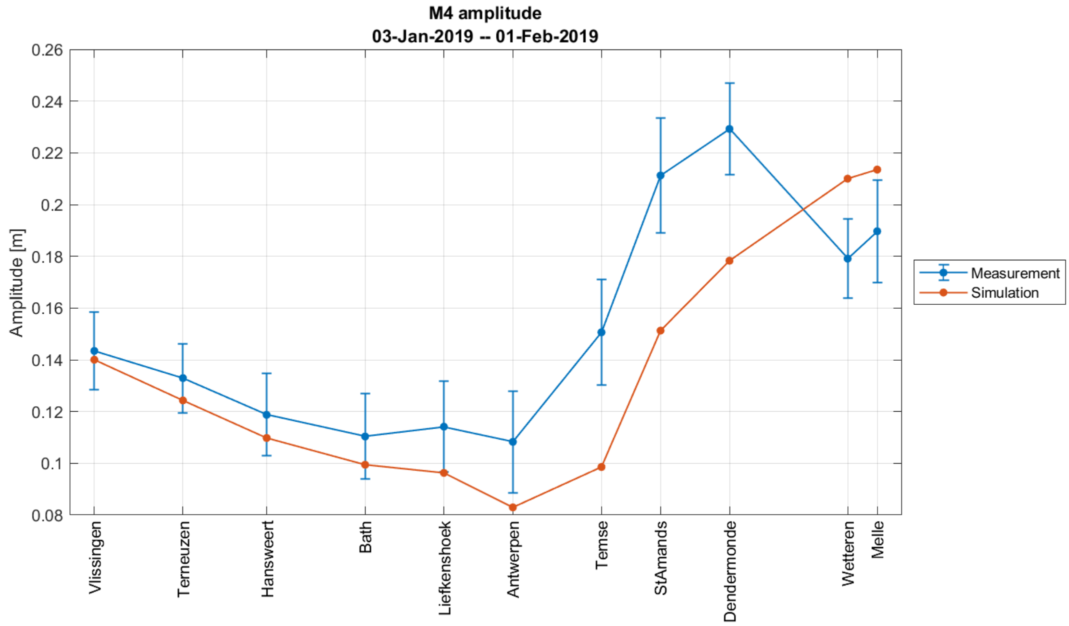

Figure 27 – Comparison between observed and modelled M4 amplitude for the validation run.

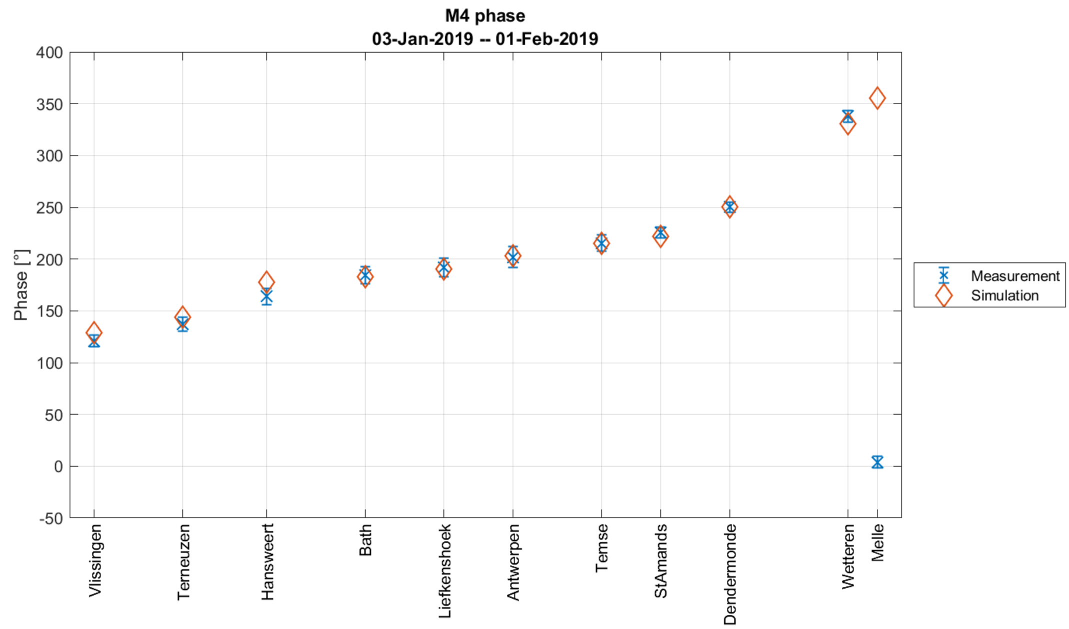

Figure 28 – Comparison between observed and modelled M4 phase for the validation run.

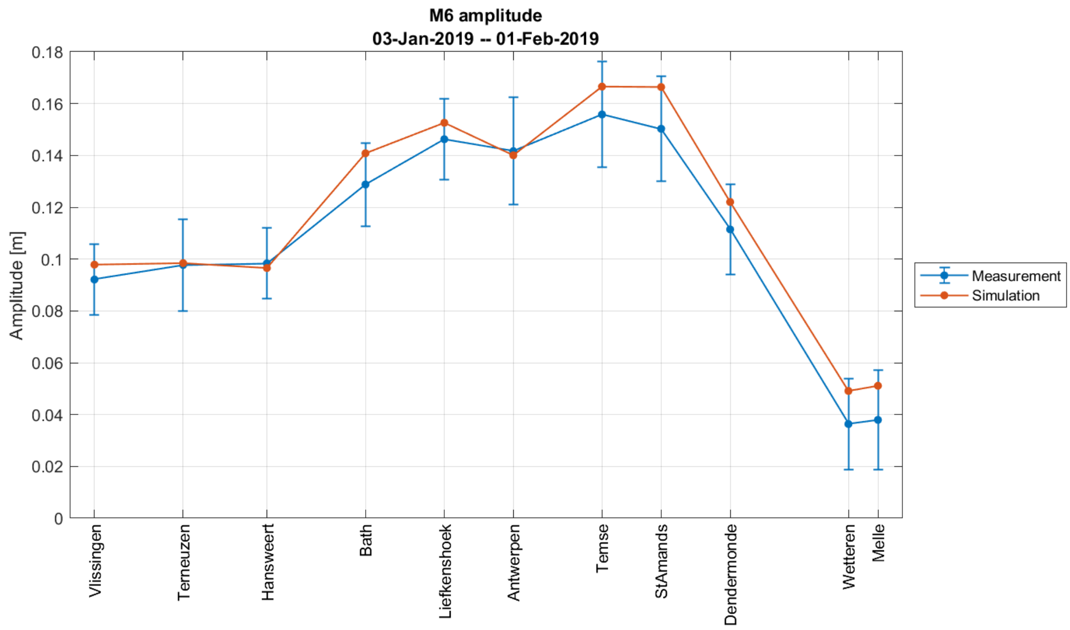

Figure 29 – Comparison between observed and modelled M6 amplitude for the validation run.

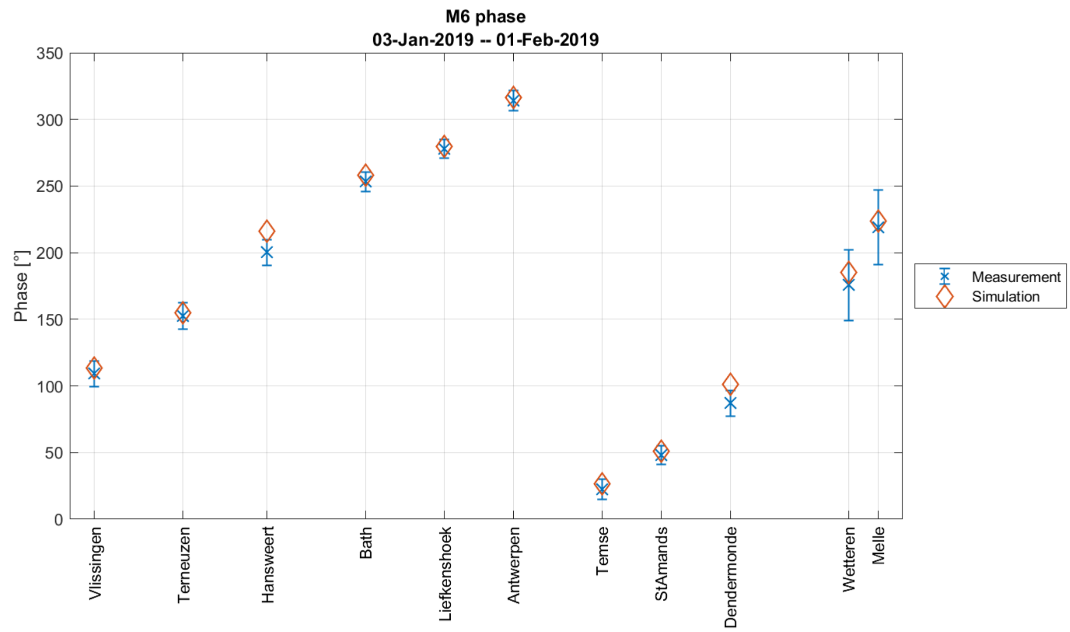

Figure 30 – Comparison between observed and modelled M6 phase for the validation run.

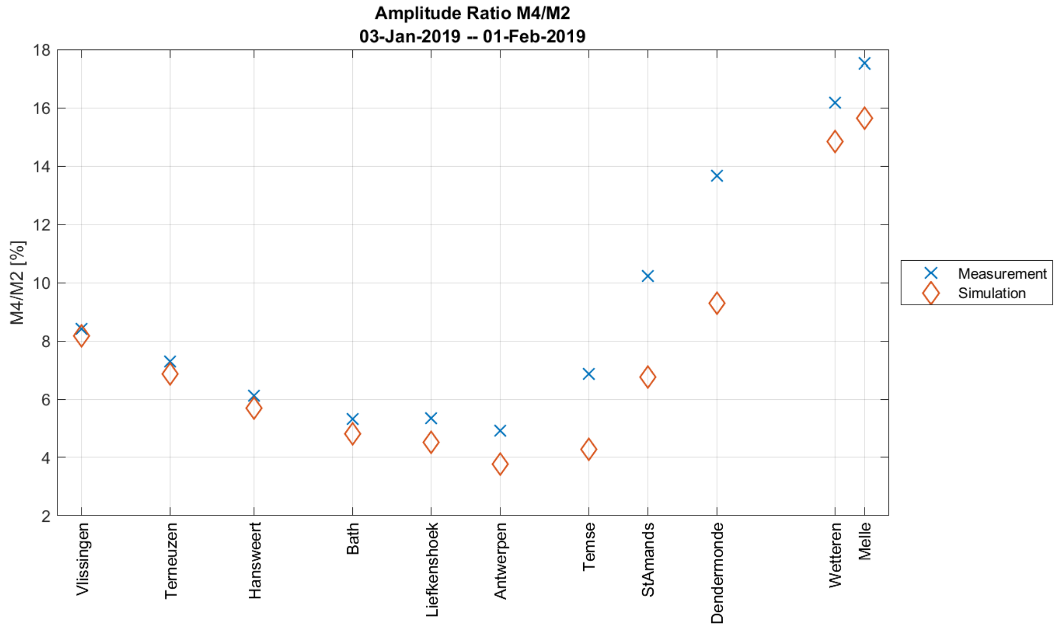

Figure 31 – Comparison between observed and modelled M4/M2 amplitude ratio for the validation run.

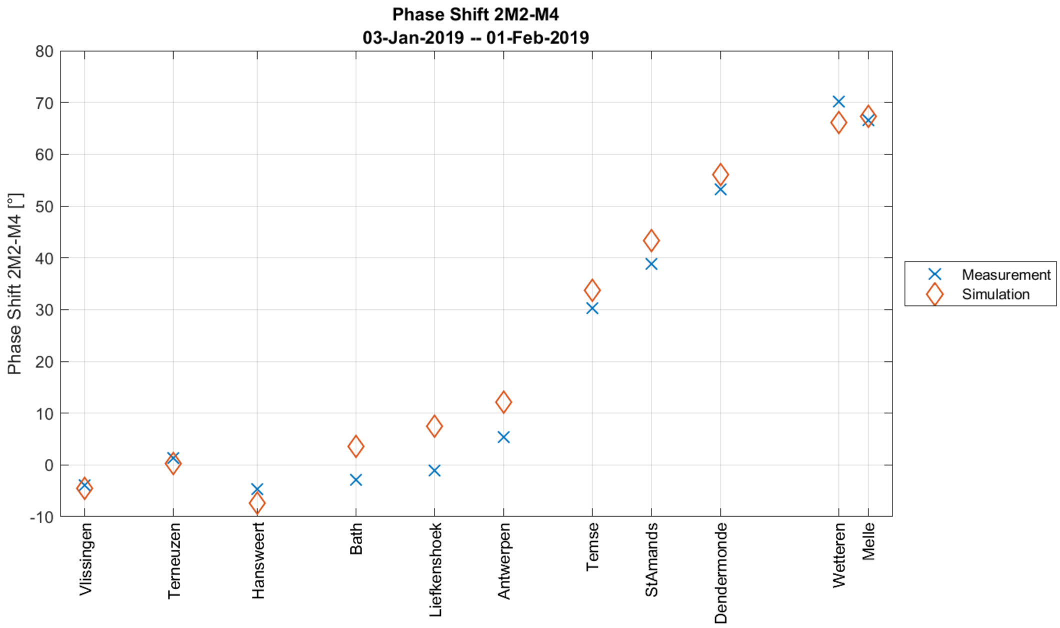

Figure 32 – Comparison between observed and modelled 2M2-M4 phase difference for the validation run.

DEPARTMENT **MOBILITY & PUBLIC WORKS**
Flanders hydraulics Research

Berchemlei 115, 2140 Antwerp
T +32 (0)3 224 60 35
F +32 (0)3 224 60 36
waterbouwkundiglabo@vlaanderen.be
www.flandershydraulicsresearch.be